Supporting Information

Triboelectric behaviour of selected MOFs in contact with metals

Andris Šutka,*[a] Fa-Kuen Shieh,[b] Martynas Kinka,[c] Linards Lapčinskis,[a] Chien-Chun Chang,[b] Phuc Khanh Lam,[b] Kaspars Pudzs,[d] and Osvalds Verners [a]

[a] Institute of Materials and Surface Engineering, Faculty of Materials Science and Applied Chemistry, Riga Technical University, Paula Valdena 3/7, Riga 1048, Latvia

[b] Department of Chemistry, National Central University, Taoyuan 32001, Taiwan

[c] Faculty of Physics, Vilnius University, Sauletekio av. 3, 10257 Vilnius, Lithuania

[d] Institute of Solid State Physics, University of Latvia, Kengaraga 8, Riga 1063, Latvia

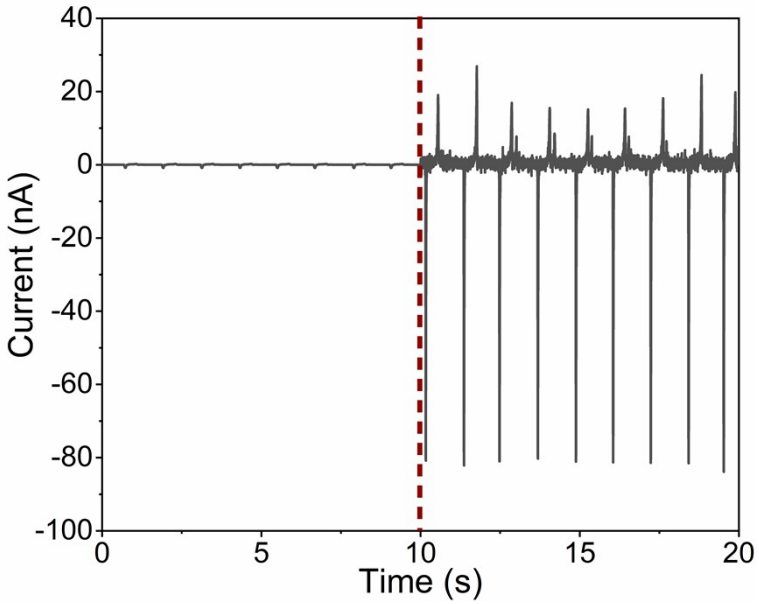

Figure S1. Current peaks generated during contact-separation of Al electrode against glass (left) and UiO-66-NH_2 covered glass (right).

Table S1. The pseudopotentials from http://pseudopotentials.quantum-espresso.org/legacy_tables/ps-library employed for DFT calculation of the work functions of MOFs.

Element	Used pseudopotential
Zn	Zn.pbe-dnl-kjpaw_psl.1.0.0.UPF
O	O.pbe-n-kjpaw_psl.1.0.0.UPF
C	C.pbe-n-kjpaw_psl.1.0.0.UPF
H	H.pbe-kjpaw_psl.1.0.0.UPF

Zr	Zr.pbe-spn-kjpaw_psl.1.0.0.UPF
N	N.pbe-n-kjpaw_psl.1.0.0.UPF

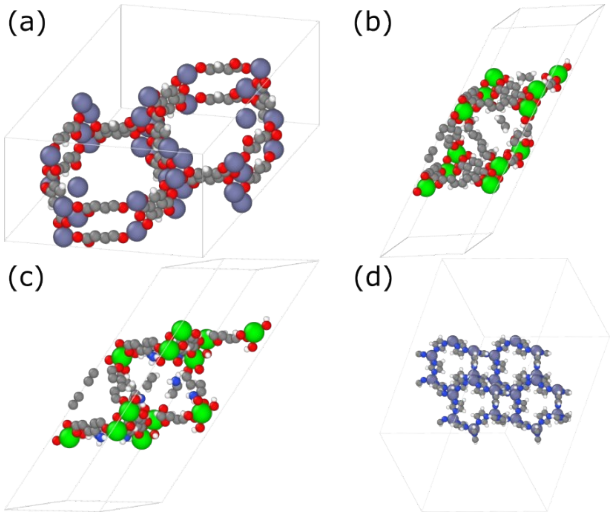

Figure S2. Geometries of 2-dimensionally periodic unit cells of (a) MOF-74 (adapted from [https://doi.org/10.1021/ja045123o]), (b) Ui-66 (adapted from [https://github.com/WMD-group/Crystal_structures/tree/master/MOFs/UiO]), (c) UiO-66-NH2 (adapted from [https://doi.org/10.1002/anie.201505461]), and (d) ZIF-8 (adapted from [https://doi.org/10.1039/B912997A]) (● – O, ● – H, ● – C, ● – N, ● – Zn, ● – Zr)

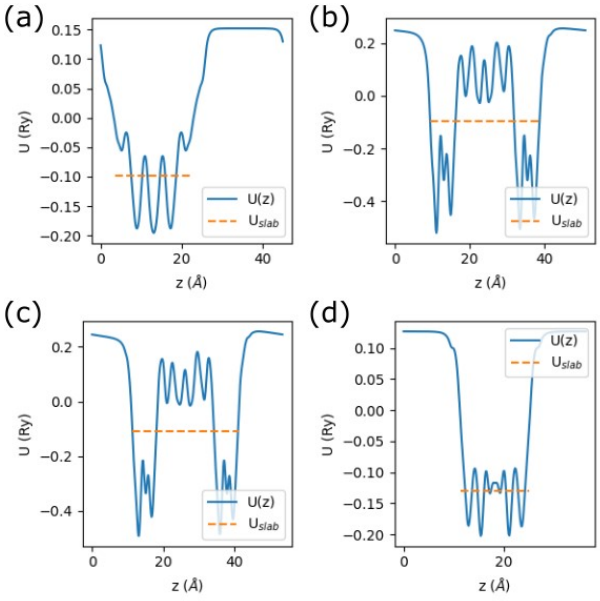

Figure S3. Surface-perpendicular distribution of electrostatic potential of 2-dimensionally periodic unit cells of (a) MOF-74, (b) Ui-66, (c) UiO-66-NH2, and (d) ZIF-8.

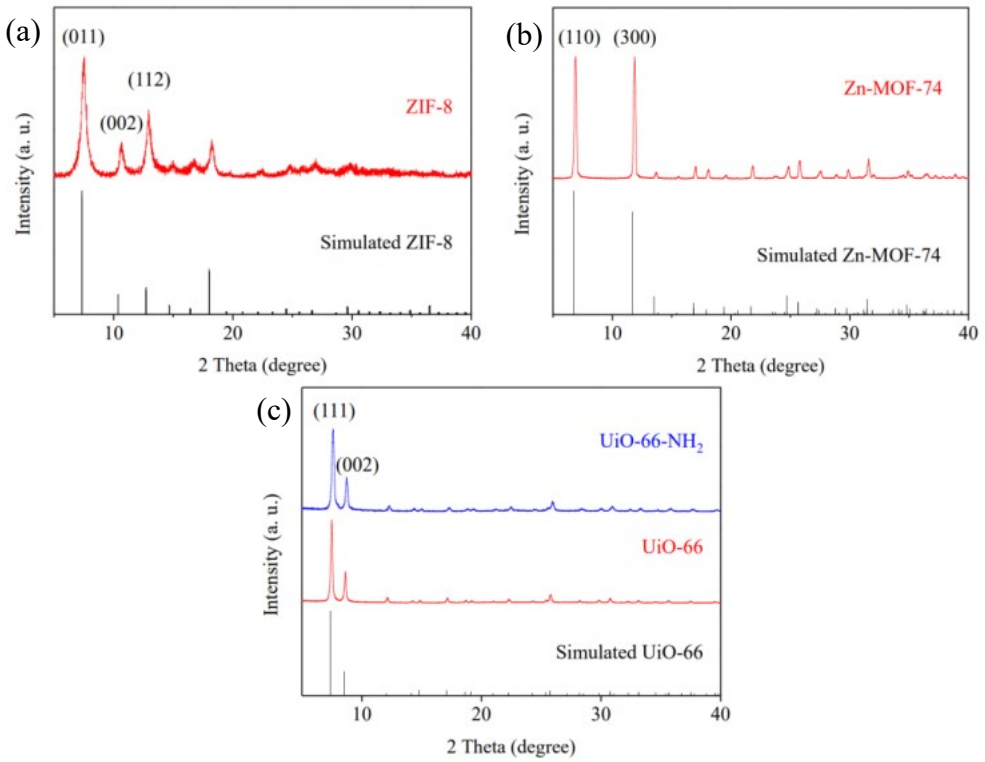

Figure S4. PXRD patterns of the synthesized and simulated (a) ZIF-8, (b) Zn-MOF-74, and (c) UiO-66, UiO-66-NH_2.

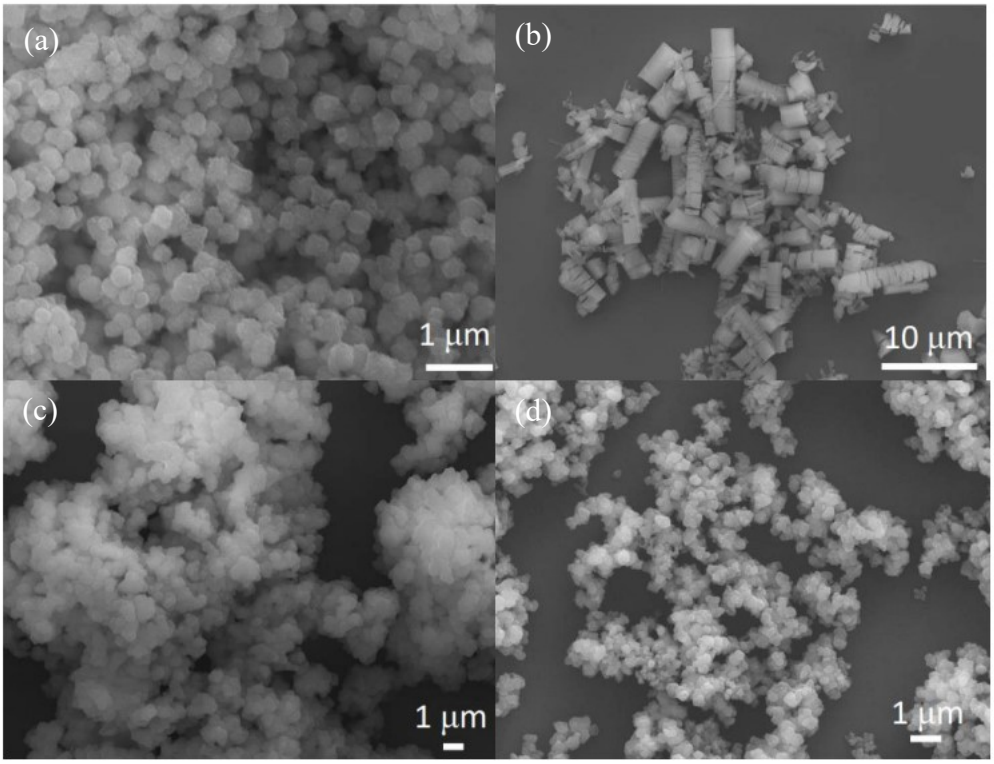

Figure S5. SEM images of (a) ZIF-8, (b) Zn-MOF-74, (c) UiO-66, and (d) UiO-66-NH_2.

Table S2. The Ra surface roughness of electrodes used for contact-separation tests against MOF coatings.

Electrode	Ra surface roughness, nm
Ag	62.0 ± 15.4
Ti	55.4 ± 16.1
Ni-Mo	25.1 ± 1.8
Al	14.6 ± 1.2

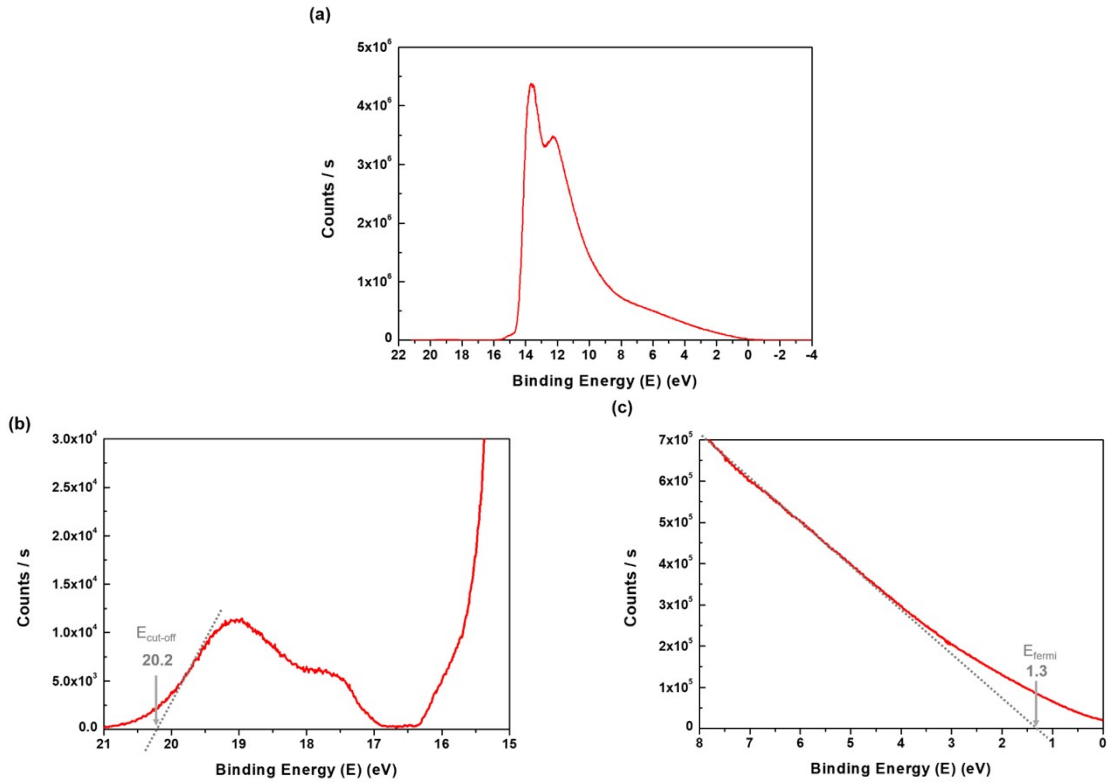

Figure S6. (a) Ultraviolet Photoelectron spectra (UPS) showing the binding energy of ZIF-8 (UV source is He I, 21.2 eV). The magnified version of UPS spectra (b) presenting the $E_{cut\text{-}off}$ as 20.2 eV and (c) displaying the E_{fermi} as 1.3 eV.

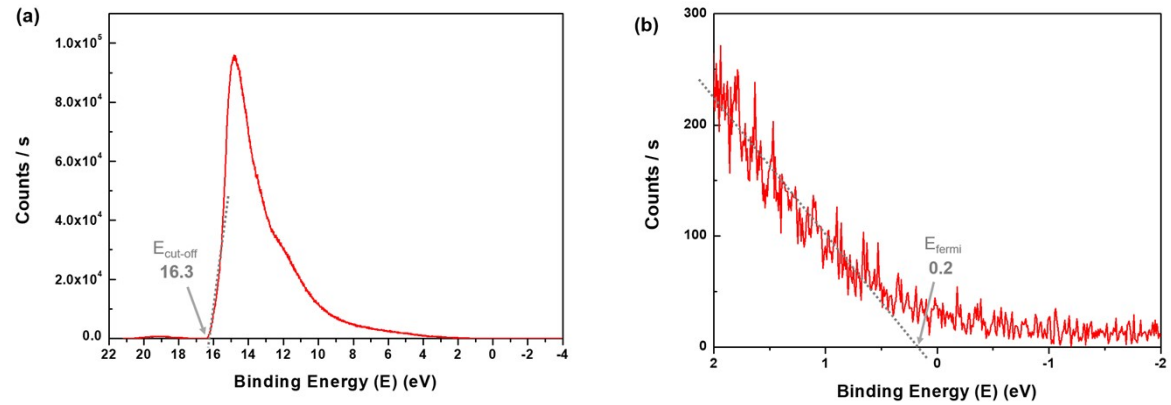

Figure S7. (a) Ultraviolet Photoelectron spectra (UPS) showing the binding energy of Zn-MOF-74 (UV source is He I, 21.2 eV) and the $E_{cut\text{-}off}$ as 16.3 eV. (b) The magnified version of UPS spectra displaying the E_{fermi} as 0.2 eV.

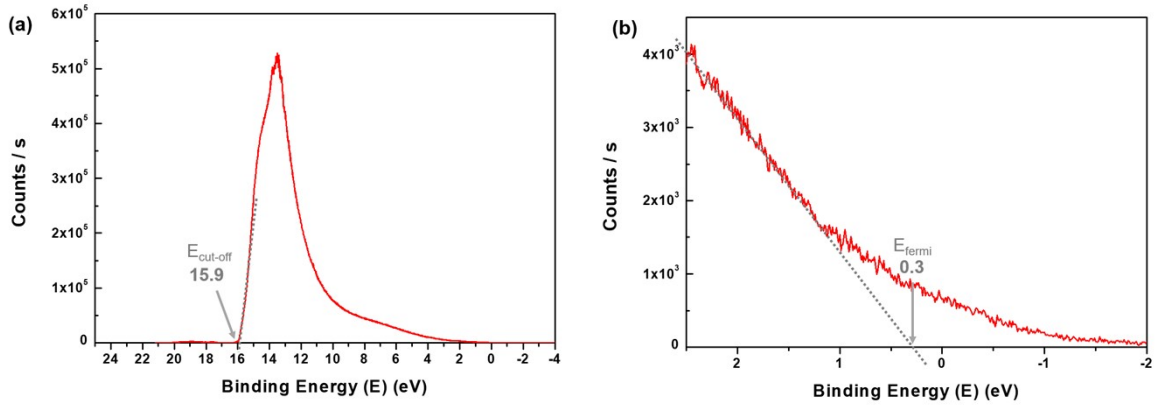

Figure S8. (a) Ultraviolet Photoelectron spectra (UPS) showing the binding energy of UiO-66 (UV source is He I, 21.2 eV) and the $E_{cut\text{-}off}$ as 15.9 eV. (b) The magnified version of UPS spectra displaying the E_{fermi} as 0.3 eV.

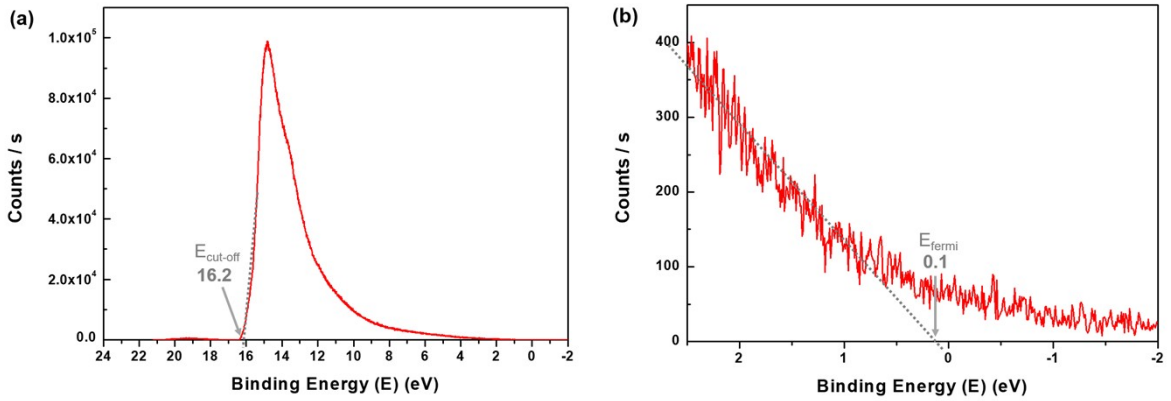

Figure S9. (a) Ultraviolet Photoelectron spectra (UPS) showing the binding energy of UiO-66-NH_2 (UV source is He I, 21.2 eV) and the $E_{cut\text{-}off}$ as 16.2 eV. (b) The magnified version of UPS spectra displaying the E_{fermi} as 0.1 eV.

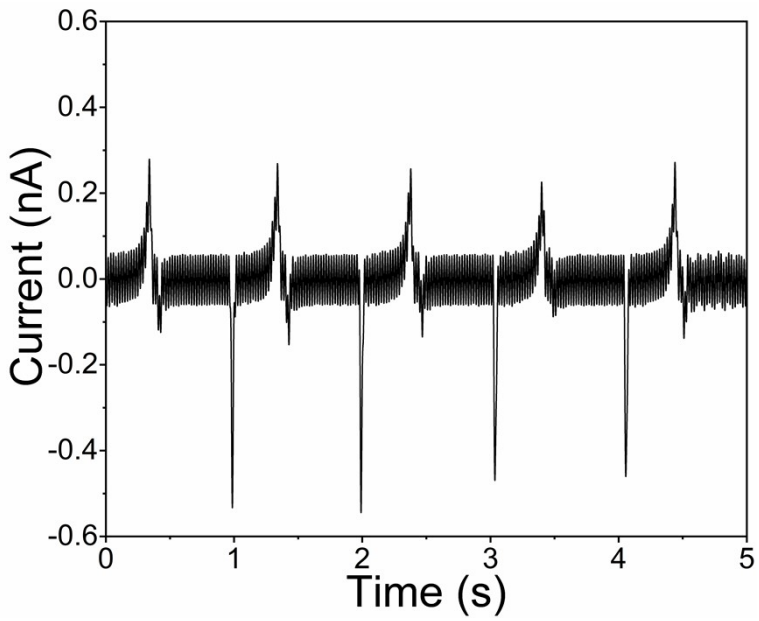

Figure S10. Current peaks of Al electrode in non-contact mode after contact with UiO-66.

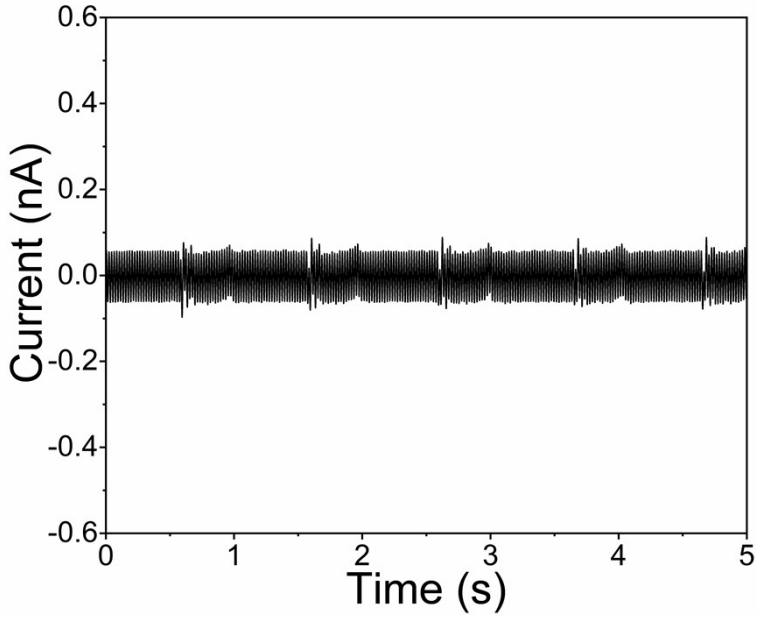

Figure S11. Current peaks of briefly grounded Al electrode in non-contact mode after contact with UiO-66.

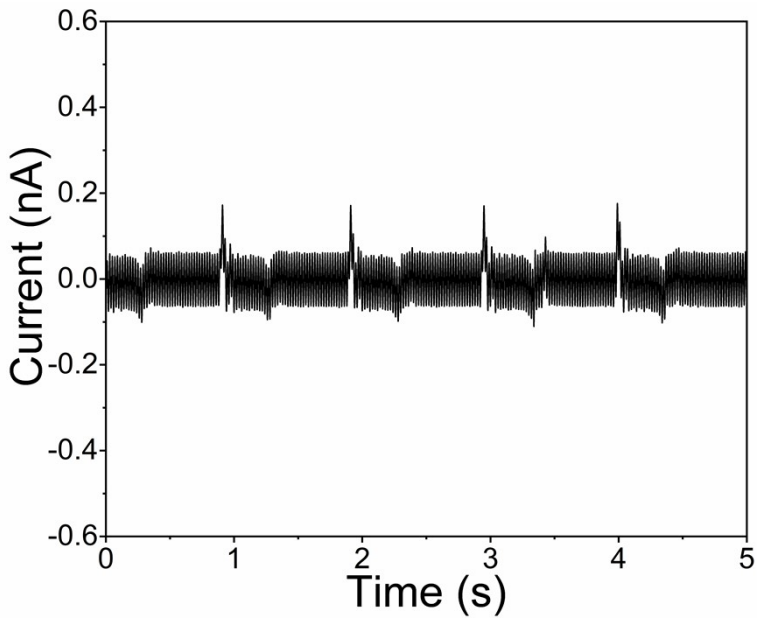

Figure S12. Current peaks of Al electrode in non-contact mode after contact with PDMS.

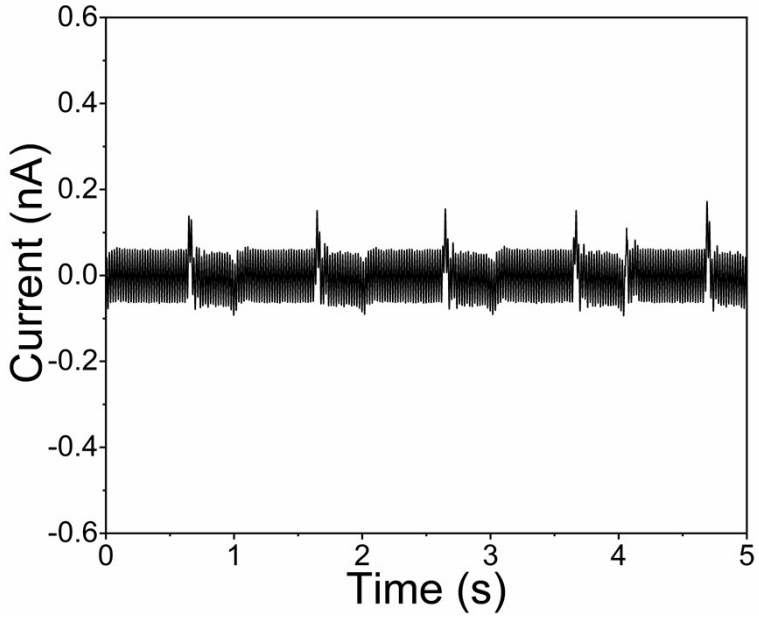

Figure S13. Current peaks of briefly grounded Al electrode in non-contact mode after contact with PDMS.